Journal of Hazardous Materials 166 (2009) 1339–1343

Contents lists available at ScienceDirect

Journal of Hazardous Materials

journal homepage: www.elsevier.com/locate/jhazmat

Entrapment of iron nanoparticles in calcium alginate beads for groundwater remediation applications

Achintya N. Bezbaruah[a,*], Sita Krajangpan[a], Bret J. Chisholm[b], Eakalak Khan[a], Juan J. Elorza Bermudez[a,c]

[a] Civil Engineering Department, North Dakota State University, Dept 2470, P.O. Box 6050, Fargo, ND 58108, USA
[b] Center for Nanoscale Science and Engineering, North Dakota State University, Fargo, ND 58102, USA
[c] Department of Civil Engineering, North Dakota State University from University of Burgos, Burgos 09001, Spain

ARTICLE INFO

Article history:
Received 29 October 2008
Received in revised form 9 December 2008
Accepted 10 December 2008
Available online 14 December 2008

Keywords:
Iron nanoparticle
Alginate beads
Entrapment
Nitrate
Groundwater remediation

ABSTRACT

Zero-valent iron nanoparticles (nZVI) have been successfully entrapped in biopolymer, calcium (Ca)-alginate beads. The study has demonstrated the potential use of this technique in environmental remediation using nitrate as a model contaminant. Ca-alginate beads show promise as an entrapment medium for nZVI for possible use in groundwater remediation. Based on scanning electron microscopy images it can be inferred that the alginate gel cluster acts as a bridge that binds the nZVI particles together. Kinetic experiments with 100, 60, and 20 mg NO_3^--N L^{-1} indicate that 50–73% nitrate-N removal was achieved with entrapped nZVI as compared to 55–73% with bare nZVI over a 2-h period. The controls ran simultaneously show little NO_3^--N removal. Statistical analysis indicates that there was no significant difference between the reaction rates of bare and entrapped nZVI. The authors have shown for the first time that nZVI can be effectively entrapped in Ca-alginate beads and no significant decrease in the reactivity of nZVI toward the model contaminant (nitrate here) was observed after the entrapment.

Published by Elsevier B.V.

1. Introduction

In recent years, zero-valent iron (Fe^0) nanoparticles (nZVI) have been used for the removal of various groundwater contaminants including chlorinated compounds [1,2], pesticides [3–5], heavy metals [6,7], and explosives [8,9] in water. Advantages of nZVI over other zero-valent iron (ZVI) such as microparticles (mZVI) and iron filings include higher reactive surface area (25–54 m^2 g^{-1} for nZVI [5,10,11] and 1 m^2 $g^{-1}$for mZVI [5]), faster and more complete reactions, and injectability into the aquifer [12–14].

Because of smaller particle size and relatively higher dispersibility (as compared to other ZVI materials), nZVI becomes mobile in the aquifer [12,13,15]. Further, if present in higher concentration, nZVI tend to agglomerate due to magnetic and van der Waals forces and form larger particles that settle into aquifer media pores. Agglomerated particles have decreased specific surface and hence lose the very advantage individual nZVI has. The higher mobility, agglomeration, and oxidation by non-target compounds in groundwater remain as major challenges for nZVI use for groundwater remediation [16]. To overcome these problems, this paper presents work done to entrap nZVI in a porous polymeric hydrogel.

Entrapment within calcium (Ca)-alginate beads is one of the most common methods for immobilizing living cells in food and beverage industries [17,18]. Ca-alginate hydrogels and microbeads are also used for drug delivery [19]. In addition, Ca-alginate entrapped bacterial and fungal cells have been used to remediation heavy metals [20–22] and nitrogen [23,24]. Alginate entrapped surfactants [25], activated carbon [26], and metal hydroxides (Fe^{3+} and Ni^{2+}) [27] have been used to recover/treat aqueous copper, organics, and arsenic, respectively. Immobilization of cells in Ca-alginate is a simple and cost effective technique [23]. Porosity in Ca-alginate allows solutes to diffuse into the beads and come in contact with the entrapped cells [28]. Moreover, alginate is nontoxic, biodegradable, and nonimmunogenic, and produces thermally irreversible and water insoluble gels [29,30].

The objective of this paper is to demonstrate that iron nanoparticles can be effectively entrapped in a biopolymer matrix (alginate) without significant reduction in their reactivity. nZVI have been entrapped within alginate beads to reduce their mobility/sedimentation in the aquifer. Effectiveness of the entrapped nanoparticles in contaminant remediation was examined with nitrate as the test contaminant.

* Corresponding author. Tel.: +1 701 231 7461; fax: +1 701 231 6185.
E-mail address: a.bezbaruah@ndsu.edu (A.N. Bezbaruah).

0304-3894/$ – see front matter. Published by Elsevier B.V.
doi:10.1016/j.jhazmat.2008.12.054

2. Materials and methods

2.1. Chemicals

Iron(II) sulfate heptahydrate ($FeSO_4 \cdot 7H_2O$, 99%, Alfa Aesar), sodium borohydride ($NaBH_4$, 98%, Aldrich), calcium chloride ($CaCl_2$, ACS grade, BDH), sodium alginate (production grade, PFALTZ&BAUER), methanol (production grade, BDH), and ethanol (ACS grade, Mallinckrodt Chemicals) were used as received.

2.2. Synthesis of nZVI and entrapment of nZVI

Nanoparticles were synthesized by borohydride reduction of ferrous iron [5,11,31]. The method for cell entrapment in alginate [32] was modified for nZVI. One gram of sodium alginate was dissolved in 50 mL deoxygenated deionized water (DDW) at room temperature ($22 \pm 2\,^{\circ}C$). The alginate–water mixture was stirred until complete dissolution was achieved (~20–30 min) and left at room temperature for ~30 min to allow the air/gas bubbles generated due to mixing to escape (to ensure that the alginate beads did not float in the aqueous solution). The alginate solution (2%, w/v) was gently mixed with 1 g of nZVI. The mixture was promptly dropped into a 3.5% (v/v) deoxygenated aqueous solution of $CaCl_2$ at room temperature using a peristaltic pump (Masterflex, Cole Parmer, 0.5 mm ID tubing, 2.5 mL min^{-1} flow rate). As soon as the alginate drops came in contact with the $CaCl_2$ solution, Ca-alginate gel beads were formed. To ensure that almost all nZVI were entrapped the alginate solution and nZVI mixture was continuously stirred with a glass rod. The leftover nZVI (in the beaker and the pump tubing) was accounted for by measuring them after washing them with deoxygenated water [33]. The average amount leftover (not entrapped) was found to be 0.0019 g (out of total 1 g) which corresponds to an error of 0.19%. The gel beads were retained in the deoxygenated $CaCl_2$ solution for ~9 h for hardening and then washed with DDW. A minimum of 6 h hardening ensures that the beads allow optimal diffusion of substrates into and out of them [32,34].

2.3. Nitrate degradation kinetics experiments

Batch nitrate degradation experiments were performed in anaerobic reactors made of 500 mL commercial grade polyethylene terephthalate bottles fitted with sleeve type silicone septum seal. Initial concentrations of 20, 60, and 100 mg NO_3^--N L^{-1} (in 450 mL DDW) were tried. The initial concentrations were kept higher than the maximum contaminant level (MCL) of NO_3^--N (10 mg L^{-1}). Ca-alginate entrapped nZVI (1.0 g) were added to each reactor. The reactors were rotated end-over-end at 28 rpm in a custom made shaker. Aliquots were withdrawn periodically (at 0, 15, 30, 45, 60, 90, 120, 240, 480, 720, 960, 1200, and 1440 min) and analyzed for nitrate. The samples were collected using a syringe fitted with a needle. The needle was inserted through the silicon septum and withdrawn after sample collection. This sample collection technique ensured that the reactor remained anaerobic. The collected samples were filtered using a syringe filter (0.02 μm) which effectively retained all nZVI (35 nm diameter). Controls with nitrate in DDW but no nZVI were run. Similar experiments were conducted with bare nZVI. All experiments were conducted in triplicates.

2.4. nZVI characterization and analytical methods

nZVI particle size was analyzed through transmission electron microscopy (TEM, JEOL JEM-100CX II). Scanning electron microscopy with X-ray microanalysis (SEM/EDX, JEOL JSM-6300) and TEM were used to observe bare nZVI and Ca-alginate entrapped nZVI surface morphology [24]. The specific surface area of bare nZVI was measured with a micromeritics analyzer (ASAP 2000, GA) using Brunauer–Emmett–Teller (BET) gas adsorption with N_2. The concentration of NO_3^--N was measured using a nitrate electrode with reference to a Ag/AgCl electrode (SympHony, VWR) [33].

3. Results and discussion

3.1. Characteristics of bare nZVI

Analysis of TEM images (not shown) indicates that nZVI particle size ranges from 10 to 100 nm with an average size of 35 nm (Fig. 1). TEM image shows clusters of agglomerated nZVI. This agglomeration limits the availability of surface area on the particle and hence available reactive surface area for contaminant degradation [35]. A higher magnification TEM image shows a ~2.5 nm of oxide shell around the nZVI core. Similar nZVI core/shell geometry and the shell forms have been reported earlier [5,11,15,36,37].

3.2. Characteristics of entrapped nZVI

SEM (Fig. 2b–d) and TEM (Fig. 2e and f) images are used to qualitatively understand the morphology inside the alginate beads. The dispersibility and location of nZVI inside the alginate bead are also investigated from these images. One of the images (Fig. 2d) shows heterogeneity of pore size in the alginate beads because crosslinking between Ca^{2+} and alginate is not uniform throughout the bead. In some parts, Ca-alginate formed densely and entrapped more nanoparticles. In higher density areas there is a possibility of nZVI agglomeration and hence reduction in their reactive surface area. The higher magnification TEM images (Fig. 2e and f) confirm high agglomeration of nZVI in parts of the beads. Further, SEM analysis revealed that the bead surface has undulations, folds, and pores (also reported by Benerjee et al. [38]). Benerjee et al. [38] reported the pore size in similar alginate beads to be 3.17–5.07 nm. Reported small pore size ensures retention of nZVI (diameter >10 nm) within the alginate beads.

3.3. Nitrate degradation studies

Experiments were conducted to compare the effectiveness of bare nZVI and entrapped nZVI in nitrate removal at three initial concentrations without any pH adjustment (Fig. 3a–c). With bare nZVI, the NO_3^--N concentration decreased from 100, 60, and 20 mg L^{-1} to 27 mg L^{-1} (73% reduction), 23 mg L^{-1} (62%), and 9 mg L^{-1} (55%), respectively, over a 2-h period. Though the batch studies were continued for 24 h, this paper reports the results for the initial

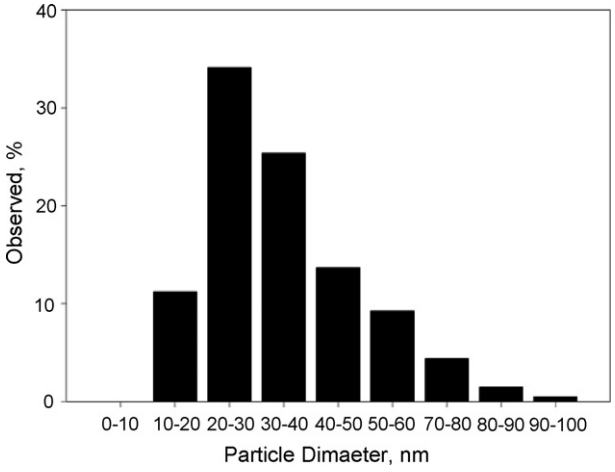

Fig. 1. Particle size distribution of synthesized nZVI. The particle size varied between 10 and 100 nm with an average value of 35 nm.

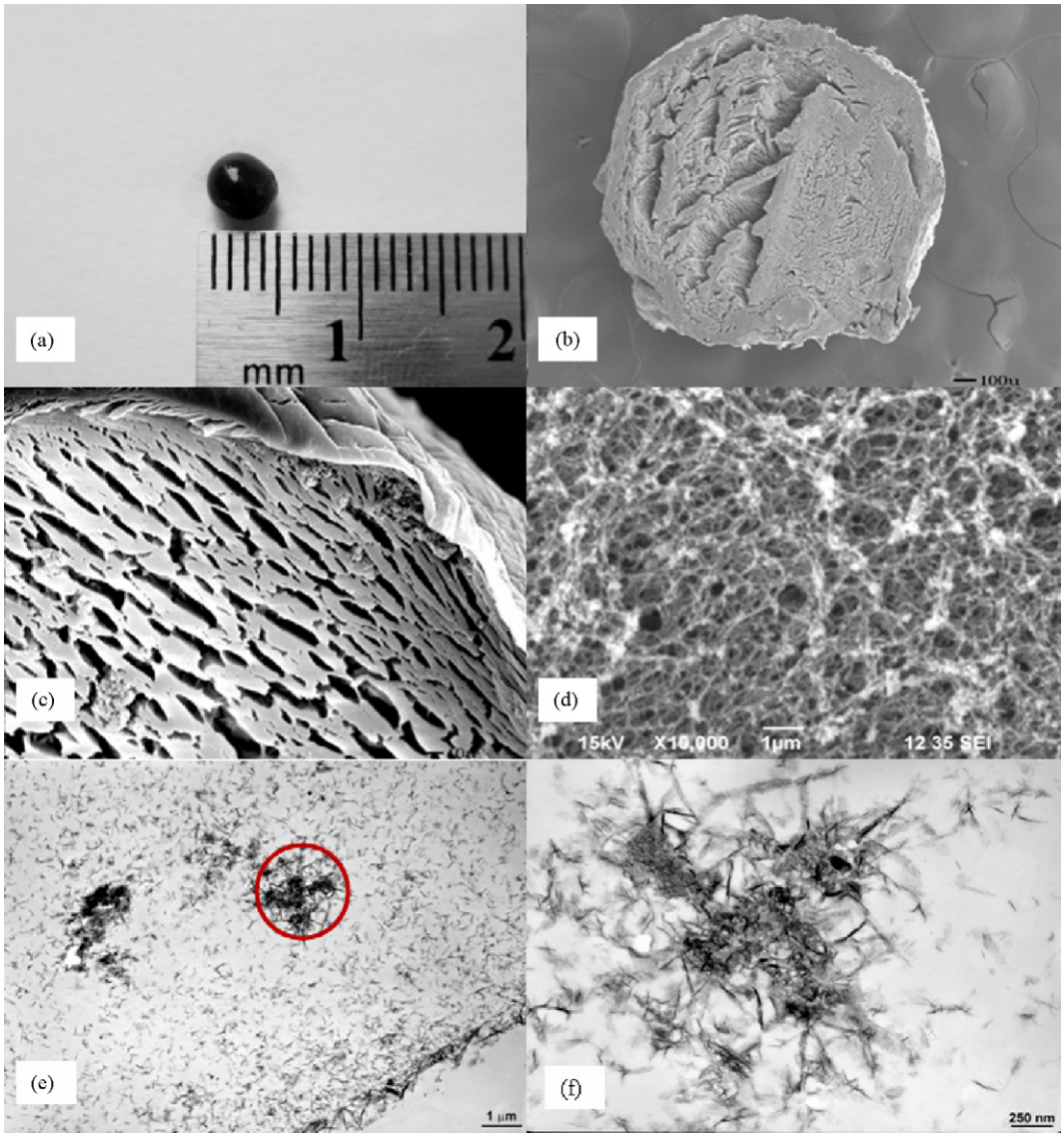

Fig. 2. (a) An alginate bead with entrapped nZVI, (b) SEM image of alginate bead. The section was taken through the center of the bead, (c) SEM image of alginate bead surface after nZVI entrapment, (d) higher magnification of SEM image (b) bead interior with entrapped nZVI, (e) TEM image of Ca-alginate bead section shown in (d). Agglomeration/concentration of nZVI can be observed. Non-uniform crosslinking within the Ca-alginate bead had led to cluster formation and high agglomeration/concentration of nZVI, (f) blow-up image of the circled area in (e). Nanoparticles are agglomerated/concentrated more in certain area rather than being uniformly distributed throughout the bead.

2-h period only as the degradation curve leveled off beyond that time and no significant NO_3^--N reduction was observed apparently because of nZVI mass limitation. The slightly lower or similar NO_3^--N reductions were observed with entrapped nZVI than with bare nZVI for the same initial concentrations and the same reaction time. The initial NO_3^--N of 100, 60, and 20 mg L^{-1} reduced to 27 mg L^{-1} (73%), 26 mg L^{-1} (57%), and 10 mg L^{-1} (50%), respectively, with entrapped nZVI. Nitrate degradation by bare nZVI and entrapped nZVI followed first-order reaction for all concentrations. The first two data points (0 and 15 min) were not used in reaction rate calculations as there was also an absorption (by alginate) component involved. The reaction rate constants (k) and the coefficient of determination (R^2) of the fit are summarized in Table 1.

For entrapped nZVI, a marked drop in nitrate concentration during the first 15 min was observed as also in the control (Ca-alginate beads only). This initial drop in nitrate in the entrapped systems is a physical phenomenon. The initial drop in nitrate can be attributed to sorption into the Ca-alginate beads due to the NO_3^--N gradient that existed between the aqueous solution and the beads. Similar substrate sorption by Ca-alginate beads has been reported by Hill and Khan [24] and Thompson [5].

NO_3^--N reduction by entrapped nZVI was observed to be slightly lower compared to bare nZVI in some cases (Fig. 3a–c). However, two-way analysis of variance test on the reaction rate data indicates that there is no significant difference between the reaction rates of bare nZVI and entrapped nZVI ($\alpha = 0.05 < p$-value = 0.142). Complete

Table 1
First-order rate constants for NO_3^--N reduction.

Iron type	Initial NO_3^--N concentration (mg L^{-1})	Reaction rate constant (h^{-1})	R^2
Bare nZVI	100	0.6547	0.9994
	60	0.4769	0.9966
	20	0.3990	0.9964
Entrapped nZVI	100	0.6465	0.9988
	60	0.4268	0.9986
	20	0.3716	0.9912

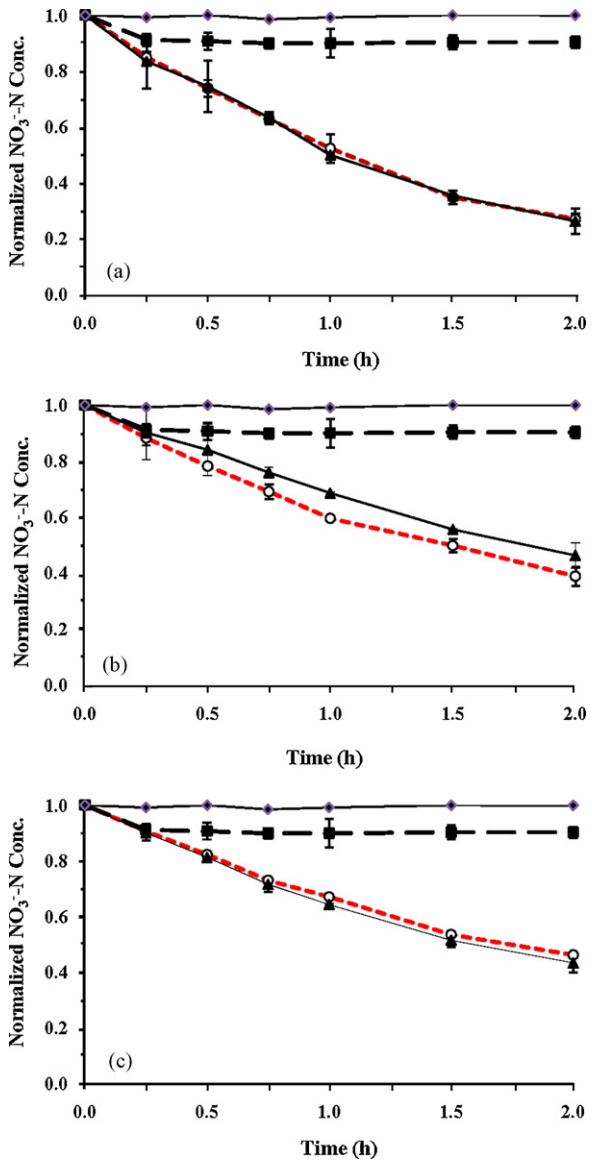

Fig. 3. (a) Reduction of NO_3^--N by bare nZVI and Ca-alginate entrapped nZVI over time. Initial NO_3^--N concentration was 100 mg L^{-1}. (b) reduction of NO_3^--N by bare nZVI and Ca-alginate entrapped nZVI over time. Initial NO_3^--N concentration was 60 mg L^{-1}, (c) reduction of NO_3^--N by bare nZVI and Ca-alginate entrapped nZVI over time. Initial NO_3^--N concentration was 20 mg L^{-1}. The vertical error bars indicate ±standard deviations. The straight lines joining the data points are for ease of reading only and do not represent trend lines. (–○– Bare nZVI, –▲– entrapped nZVI, –■– control, –♦– blank).

nitrate degradation was not achieved either with bare or entrapped nZVI probably because nZVI dose used in the experiments was low. More experiments were not conducted with higher nZVI dose since this study focused on the entrapment of nZVI in alginate beads and the effectiveness of entrapped nZVI relative to bare nanoparticles.

The authors expected some reduction in nitrate degradation rate due to the presence of alginate coating on the nZVI and hence diffusion limitations. It is apparent from the results that there was no solute diffusion limitation. Nitrate diffusion in alginate beads is non-Fickian in nature and depends on the concentration of alginate and extent of crosslinking of calcium ion [34]. The alginate beads used in this experiment were gelled for more than 6 h. Therefore, they should have reached the optimal nitrate diffusion characteristics [32] and should not restrict substrate (nitrate here) diffusion through them [34].

The results clearly indicate that the reactivity of entrapped nZVI was comparable to bare nZVI. Reduced mobility of iron nanoparticles can be achieved through entrapment in Ca-alginate. With further improvement in dispersibility of the nZVI within the beads, the alginate entrapment technique may possibly offer a way to effectively use nZVI in many groundwater remediation situations. Iron nanoparticles are known to degrade a broad range of contaminants including chlorinated compounds, heavy metals, pesticides, and explosives [1–9] and alginate beads are known to allow diffusion of a wide range of compounds [39–41]. Four chlorinated methanes, six chlorinated benzenes, two pesticides, five organic dyes, four heavy metals, three trihalomethanes, six chlorinated ethenes, three polychlorinated hydrocarbons, four inorganic anions, TNT, and NDMA are reported to be remediated (or transformed) by nZVI [14]. Recently Thompson [5] demonstrated treatability of high concentration alachlor with nZVI. Further, LaGrega et al. [42] lists 22 organic and 16 inorganic contaminants treatable with ZVI. The combined alginate–nZVI system is, therefore, expected to be effective for a similar wide range of contaminants. The entrapped nZVI will have the advantage of being stationary in the aquifer under dynamic groundwater conditions as compared to the bare particles.

4. Conclusions

The results from this study indicate that nZVI entrapment in a biopolymer may increase their overall efficacy of for groundwater remediation. The authors have shown for the first time that nZVI can be effectively entrapped in Ca-alginate beads and reactivity of entrapped nZVI toward a model contaminant (nitrate here) was comparable to that of bare nZVI. The reduction in nitrate concentration using bare nZVI and entrapped nZVI were 55–73% and 50–73%, respectively, over a 2-h period. Ca-alginate can be used as the entrapment medium for nZVI to make the nanoparticles relatively stationary in aqueous media (e.g., groundwater). Thus, the mobility and settlement problems associated with bare nZVI can be overcome and alginate entrapped nZVI can be effectively used in permeable reactive barriers for groundwater remediation.

Acknowledgments

Grants from USGS/North Dakota Water Resources Research Institute and North Dakota State University (NDSU) Development Foundation are thankfully acknowledged.

References

[1] Y.Q. Liu, G.V. Lowry, Effect of particle age (Fe-o content) and solution pH on NZVI reactivity: H-2 evolution and TCE dechlorination, Environ. Sci. Technol. 40 (2006) 6085–6090.
[2] R. Cheng, J.-L. Wang, W.-X. Zhang, Comparison of reductive dechlorination of *p*-chlorophenol using Fe^0 and nanosized Fe^0, J. Hazard. Mater. 144 (2007) 334–339.
[3] A.J. Feitz, S.H. Joo, J. Guan, Q. Sun, D.L. Sedlak, T.D. Waite, Oxidative transformation of contaminants using colloidal zero-valent iron, Colloid Surf. A 265 (2005) 88–94.
[4] S.H. Joo, D. Zhao, Destruction of lindane and atrazine using stabilized iron nanoparticles under aerobic and anaerobic conditions: effects of catalyst and stabilizer, Chemosphere 70 (2008) 418–425.
[5] J.M. Thompson, Chlorinated pesticide remediation using zero-valent iron nanoparticles (M.S. Thesis), North Dakota State University, Fargo, ND, 2008.
[6] D.W. Blowes, C.J. Ptacek, J.L. Jambor, In-situ remediation of Cr(VI) contaminated groundwater using permeable reactive walls: laboratory studies, Environ. Sci. Technol. 31 (1997) 3348–3357.
[7] M.J. Alowitz, M.M. Scherer, Kinetics of nitrate, nitrite, and Cr(VI) reduction by iron metal, Environ. Sci. Technol. 36 (2002) 299–306.
[8] K.B. Gregory, P. Larese-Casanova, G.F. Parkin, M.M. Scherer, Abiotic transformation of hexahydro-1,3,5-trinitro-1,3,5-triazine by FeII bound to magnetite, Environ. Sci. Technol. 38 (2004) 1408–1414.
[9] S.-Y. Oh, P.C. Chiu, B.J. Kim, D.K. Cha, Zero-valent iron pretreatment for enhancing the biodegradability of RDX, Water Res. 39 (2005) 5027–5032.

[10] S.S. Chen, H.-D. Hsu, C.-W. Li, A new method to produce nanoscale iron for nitrate removal, J. Nanopart. Res. 6 (2004) 639–647.
[11] L. Li, M. Fan, R.C. Brown, J.H. Van Leeuwen, J. Wang, W. Wang, Y. Song, Z. Zhang, Synthesis, properties, and environmental applications of nanoscale iron-based materials: a review, Crit. Rev. Env. Sci. Tech. 36 (2006) 405–431.
[12] K.L. Cantrell, D.I. Kaplan, T.W. Wietsma, Zero-valent iron for the in situ remediation of selected metals in groundwater, J. Hazard. Mater. 42 (1995) 201–212.
[13] C.B. Wang, W.-X. Zhang, Synthesizing nanoscale iron particles for rapid and complete dechlorination of TCE and PCBs, Environ. Sci. Technol. 31 (1997) 2154–2156.
[14] W.-X. Zhang, Nanoscale iron particles for environmental remediation: an overview, J. Nanopart. Res. 5 (2003) 323–332.
[15] J.E. Martin, A.A. Herzing, W. Yan, X.Q. Li, B.E. Koel, C.J. Kiely, W.-X. Zhang, Determination of the oxide layer thickness in core-shell zerovalent iron nanoparticles, Langmuir 24 (2008) 4329–4334.
[16] S. Krajangpan, L. Jarabek, J. Jepperson, B. Chisholm, A. Bezbaruah, Polymer modified iron nanoparticles for environmental remediation, Polym. Prepr. 49 (2008) 921.
[17] M. Kobaslija, D.T. McQuade, Removable colored coatings based on calcium alginate hydrogels, Biomacromolecules 7 (2006) 2357–2361.
[18] G.I. Olivas, G.V. Barbosa-Canovas, Alginate-calcium films: water vapor permeability and mechanical properties as affected by plasticizer and relative humidity, LWT-Food Sci. Technol. 41 (2008) 359–366.
[19] Y.A. Morch, I. Donati, B.L. Strand, G. Skjak-Bræk, Effect of Ca^{2+}, Ba^{2+}, and Sr^{2+} on alginate microbeads, Biomacromolecules 7 (2006) 1471–1480.
[20] Y. Lu, E. Wilkins, Heavy metal removal by caustic-treated yeast immobilized in alginate, J. Hazard. Mater. 49 (1996) 165–179.
[21] M.Y. Arıca, G. Bayramoğlu, M. Yılmaz, S. Bektaş, Ö. Genç, Biosorption of Hg^{2+}, Cd^{2+}, and Zn^{2+} by Ca-alginate and immobilized wood-rotting fungus *Funalia trogii*, J. Hazard. Mater. 109 (2004) 191–199.
[22] S. Önal, Ş.H. Baysal, G. Ozdemir, Studies on the applicability of alginate-entrapped *Chryseomonas luteola* TEM 05 for heavy metal biosorption, J. Hazard. Mater. 146 (2007) 417–420.
[23] S.L. Zala, J. Ayyer, A.J. Desai, Nitrate removal from the effluent of a fertilizer industry using a bioreactor packed with immobilized cells of *Pseudomonas stutzeri* and *Comamonas testosterone*, World J. Microb. Biot. 20 (2004) 661–665.
[24] C.B. Hill, E. Khan, A comparative study of immobilized nitrifying and co-immobilized nitrifying and denitrifying bacteria for ammonia removal from sludge digester supernatant, Water Air Soil Pollut. 195 (2008) 23–33.
[25] A. Karagunduz, Y. Kaya, B. Keskinler, S. Oncel, Influence of surfactant entrapment to dried alginate beads on sorption and removal of Cu^{2+} ions, J. Hazard. Mater. 131 (2006) 79–83.
[26] Y.-B. Lin, B. Fugetsu, N. Terui, S. Tanaka, Removal of organic compounds by alginate gel beads with entrapped activated carbon, J. Hazard. Mater. 120 (2005) 237–241.
[27] C. Escudero, N. Fiol, I. Villaescusa, J.-C. Bollinger, Arsenic removal by a waste metal (hydr)oxide entrapped into calcium alginate beads, J. Hazard. Mater. (2008), doi:10.1016/j.jhazmat.2008.08.042.
[28] G.-L. Huang, S. Zhihui, Immobilization of *Spirulina subsalsa* for removal of triphenyltin from water, Artif. Cell. Blood. Sub. 30 (2002) 293–305.
[29] N.M. Velings, M.M. Mestdagh, Physicochemical properties of alginate gel beads, Polym. Gels Netw. 3 (1995) 311–330.
[30] I.M.N. Vold, K.A. Kristiansen, B.E. Christensen, A study of the chain stiffness and extension of alginates, in vitro epimerized alginates, and periodate-oxidized alginates using size-exclusion chromatography combined with light scattering and viscosity detectors, Biomacromolecules 7 (2006) 2136–2146.
[31] Y. Liu, Y. Liu, S.A. Majetich, R.D. Tilton, D.S. Sholl, G.V. Lowry, TCE dechlorination rates, pathways, and efficiency of nanoscale iron particles with different properties, Environ. Sci. Technol. 39 (2005) 1338–1345.
[32] Z. Aksu, G. E-retli, T. Kutsal, A comparative study of copper(II) biosorption on Ca-alginate, agarose and immobilized *C. vulgaris* in a packed-bed column, Process Biochem. 33 (1998) 393–400.
[33] APHA, AWWA, WEF. Standard Methods for the Examination of Water and Wastewater, 20th ed., American Public Health Association, Washington, DC, 1998.
[34] I. Garbayo, R. Leon, J. Vigara, C. Vılchez, Diffusion characteristics of nitrate and glycerol in alginate, Colloid Surf. B. 25 (2002) 1–9.
[35] O. Schlicker, M. Ebert, M. Firth, M. Weidner, W. Wust, A. Dahmke, Degradation of TCE with iron: the role of competing chromate and nitrate reduction, Ground Water 38 (2003) 403–409.
[36] J.T. Nurmi, P.G. Tratnyek, V. Sarathy, D.R. Baer, J.E. Amonette, K. Pecher, C. Wang, J.C. Linehan, D.W. Matson, R.L. Penn, M.D. Driessen, Characterization and properties of metallic iron nanoparticles: spectroscopy, electrochemistry, and kinetics, Environ. Sci. Technol. 39 (2005) 1221–1230.
[37] K. Sohn, S.W. Kang, S. Ahn, M. Woo, S.K. Yang, Fe(0) nanoparticles for nitrate reduction: stability, reactivity, and transformation, Environ. Sci. Technol. 40 (2006) 5514–5519.
[38] A. Benerjee, D. Nayan, S. Lahiri, A new method of synthesis of iron doped calcium alginate beads and determination of iron content by radiometric method, Biochem. Eng. J. 33 (2007) 260–262.
[39] E.M. Zactiti, T.G. Kieckbusch, Potassium sorbate permeability in biodegradable alginate films: effect of the antimicrobial agent concentration and crosslinking degree, J. Food Eng. 77 (2006) 462–467.
[40] K. Vijayaraghavan, M.H. Han, S.B. Choi, Y.S. Yun, Biosorption of Reactive black 5 by *Corynebacterium glutamicum* biomass immobilized in alginate and polysulfone matrices, Chemosphere 68 (2007) 1838–1845.
[41] M.K.E. McEntee, S.K. Bhatia, L. Tao, S.C. Roberts, S.R. Bhatia, Tunable transport of glucose through ionically-crosslinked alginate gels: effect of alginate and calcium concentration, J. Appl. Polym. Sci. 107 (2008) 2956–2962.
[42] M.D. LaGrega, P.L. Buckingham, J.C. Evans, Hazardous Waste Management, McGraw Hill, New York, 2001.